

INTERNATIONAL SOCIETY FOR SOIL MECHANICS AND GEOTECHNICAL ENGINEERING



This paper was downloaded from the Online Library of the International Society for Soil Mechanics and Geotechnical Engineering (ISSMGE). The library is available here:

<https://www.issmge.org/publications/online-library>

This is an open-access database that archives thousands of papers published under the Auspices of the ISSMGE and maintained by the Innovation and Development Committee of ISSMGE.

Unravelling the anisotropy of peat

Effiler de l'anisotropie de la tourbe

Cor Zwanenburg & Frans B.J. Barends
 Delft University of Technology / GeoDelft

ABSTRACT

The paper presents a study on the origin of anisotropy in stiffness of peat encountered in triaxial cell tests. It is shown that anisotropy affects the effective stress path in an undrained triaxial cell test. Due to the fibrous nature of peat a difference in stiffness is to be expected in the direction parallel and perpendicular to the fibres. A vertical load on a sample leads to an increase in pore pressure causing a decrease in radial effective stress and therefore to a radial unloading. Tests on non pre-loaded samples show that the difference in loading and unloading stiffness also plays an important role in the anisotropy encountered in standard triaxial tests. A significant axial pre-loading increases the rate of anisotropy considerably. The difference in anisotropy found in triaxial tests retrieved at different locations and different loading conditions can be explained by radial pre-stressing of the fibres.

RÉSUMÉ

L'article présente une étude sur l'origine de la déformabilité anisotrope observée lors de tests triaxiaux. Il montre que l'anisotropie affecte le chemin de contraintes effectives lors d'un test triaxial non drainé. A cause de la nature fibreuse de la tourbe, une déformabilité différente est attendue dans les directions parallèle et perpendiculaire aux fibres. Une charge verticale sur un échantillon conduit à une augmentation de la pression de pore causant une diminution de la contrainte effective radiale et par conséquent un déchargement radial. Les tests menés sur des échantillons non-préchargés montrent que la différence de déformabilité mesurée lors du chargement et du déchargement joue aussi un rôle important sur l'anisotropie observée lors des essais triaxiaux standards. Un pré-chargement significatif augmente le taux d'anisotropie de façon considérable. La différence d'anisotropie trouvée dans les essais triaxiaux menés dans différentes conditions de chargement sur des échantillons de diverses provenances et peut s'expliquer par la pré-contrainte radiale des fibres.

1 ANISOTROPY OF PEAT

Peat originates from dead vegetation. Depending on the rate of humification peat can be considered as a fibrous, heterogeneous material. Due to the fibres material properties like stiffness will be anisotropic in character. Material models that include anisotropic behaviour are hardly available and relevant parameters are difficult to obtain. So, for practical purposes, e.g. an embankment design on a peat layer, a homogeneous isotropic material behaviour is often assumed.

Although several properties of peat might have an anisotropic nature, this paper focuses on the an-isotropy of the stiffness of peat. Here it is assumed that peat behaves cross-anisotropic. It means that there is an axis of symmetry regarding the stiffness parameters, and the stiffness in both horizontal directions is essentially different from the stiffness in the vertical direction. There are three optional causes for peat to behave anisotropic. First is anisotropy due to the structure of peat. The stiffness in the main fibre direction differs from the stiffness perpendicular to the fibres. This is known as structural anisotropy. It is assumed that the fibres are mainly orientated in the horizontal plane, which leads to a difference in stiffness in the horizontal and vertical direction. The second is a load-induced anisotropy. Since peat is a soft and compressible material the stiffness depends on the stress level or even on the rate of compression. A deviator load will induce a difference in compressibility in different directions and therefore to a difference in stiffness. The third option originates from a difference in loading and unloading conditions. True elastic behaviour is only found for very small strain rates. Exceeding this small strain rate already leads to residual deformation, [Atkinson, 2000]. In engineering practice bulk moduli, which include some plastic deformation, are used. This working method implies a difference in stiffness moduli for loading and unloading conditions. Loading an undrained soil sample in axial direction gives an ef-

fective stress increase in axial direction and a decrease in radial direction. So even for isotropic soil anisotropic behaviour can be found. According to Parry & Wroth [1981] this is known as stress anisotropy.

Standard soil investigation involves mainly vertically retrieved soil samples. Collecting soil samples horizontally even at shallow depths requires special effort. So, studying anisotropy by testing vertical and horizontally retrieved samples is rarely done. In the present study both horizontal and vertical retrieved samples are considered.

2 THEORY

Hooke's law for a cross anisotropic material holds 5 unknown parameters which cannot be determined individually from single laboratory tests, a.o. [Graham & Houlsby, 1983]. In a.o. Lings et al [2000] the following constitutive equation is proposed for linear elastic cross anisotropy.

$$\begin{bmatrix} \delta\epsilon_p \\ \delta\epsilon_q \end{bmatrix} = \begin{bmatrix} 1/K' & 1/J'_{qp} \\ 1/J'_{pq} & 1/3G' \end{bmatrix} \begin{bmatrix} \delta p' \\ \delta q \end{bmatrix} \quad (1)$$

In which:

- $\delta\epsilon_p$ = change in volume strain
- $\delta\epsilon_q$ = change in deviator strain, for axial symmetry
- $\delta\epsilon_q$ = $2/3 (\delta\epsilon_a - \delta\epsilon_r)$
- $\delta\epsilon_a$ = change in axial strain
- $\delta\epsilon_r$ = change in radial strain
- $\delta p'$ = change in isotropic effective stress
- δq = change in deviator stress
- K', J', G' = stiffness parameters according to equation 2

For cross-isotropic materials $J'_{qp} = J'_{pq} = J'$. For isotropic materials $1/J'$ reduces to 0 as J' reaches infinity. The parameters K' , J' and G' are related to the intrinsic anisotropic elastic stiffness parameters according to:

$$\begin{aligned} K' &= \frac{1}{\left[(1 - 4\nu_{vh})/E_v + 2(1 - \nu_{hh})/E_h \right]} \\ J' &= \frac{3}{2 \left[(1 - \nu_{vh})/E_v - (1 - \nu_{hh})/E_h \right]} \\ G' &= \frac{3}{4 \left[(1 + 2\nu_{vh})/E_v + (1 - \nu_{hh})/2E_h \right]} \end{aligned} \quad (2)$$

In which

E_v = Young's modulus for vertical direction
 E_h = Young's modulus for horizontal direction
 ν_{vh} = Poisson ratio for horizontal strain due to vertical strain
 ν_{hh} = Poisson ratio for horizontal strain due to horizontal strain

Using equation 1 an expression for the rise in pore pressure due to undrained loading can be found, [Zwanenburg & Barnds, 2004]:

$$-\delta\sigma_w = B \left(\delta p + \frac{K'}{J'} \delta q \right) \quad (3)$$

in which:

B = Skempton B-factor
 δp = change in isotropic total stress
 δq = change in deviatoric stress
 $\delta\sigma_w$ = change in excess pore pressure

For standard triaxial testing, with σ_b the applied load on top, it is found by definition $q = \sigma_b$ and $p = 1/3\sigma_b = 1/3 q$. For $B = 1$ it follows that:

$$-\frac{\delta\sigma_w}{\delta q} = \frac{1}{3} + \frac{K'}{J'} \quad (4)$$

The parameters K' and J' can be expressed in E_h , E_v and ν_{hh} and ν_{vh} using equations 2. Since the influence of ν_{hh} and ν_{vh} on the value for K'/J' is relatively small, E_h and E_v dominate the ratio K'/J' . For $E_h > E_v$ is found $K'/J' > 0$ while for $E_h < E_v$ is found $K'/J' < 0$. The ratio K'/J' can be expressed in the stiffness parameters used in equation 2:

$$\frac{K'}{J'} = \frac{2 \left[(1 - \nu_{vh})E_h - (1 - \nu_{hh})E_v \right]}{3 \left[(1 - 4\nu_{vh})E_h + 2(1 - \nu_{hh})E_v \right]} \quad (5)$$

Results of a triaxial test can be presented in a $p - q$ diagram, known as the total stress path, TSP. The graph $p' - q$ is known as the effective stress path, ESP. Figure 1 shows a typical TSP and ESP for undrained elastic conditions. The intercept between both paths corresponds with pore pressure inside the sample. In a standard undrained triaxial test the vertical load is increased while the radial pressure remains constant. By definition of p and q the total stress path for a standard undrained triaxial test has a slope of 1:3. In an undrained test the vertical load increase gives a pore pressure reaction as presented in equation 4. The slope of the ESP is dictated by the ratio K'/J' . For an isotropic elastic material, $K'/J' = 0$ is found. Leading to $\delta\sigma_w = \delta p$ providing a vertical ESP. If $E_v < E_h$ and, or $\nu_{vh} < \nu_{hh}$ it follows that $K'/J' > 0$. The pore pressure development exceeds the increase in p leading to a reduction in p' . A backward tilting ESP is found. For $E_v > E_h$ and, or $\nu_{hh} < \nu_{vh}$ is found $K'/J' < 0$. This leads to an increase in p' and a forward tilting ESP is found. So it can be concluded that the angle of the ESP provides information about the degree of anisotropy. For an-isotropic clay this is found experimentally [Wesley, 1975]. Other literature present-

ing measurement data of K' , J' and G' are Hird & Pierpoint [1994], [1997] for Oxford clay, Atkinson et al, [1990] on stiff London clay and Ling et al. [2000] on Gault clay. Literature in which measurements K'/J' or the horizontal and vertical stiffness of peat is studied are not known to the authors.

With α the slope of the ESP, shown by figure 1, it is found $K'/J' = -1/\alpha$. In Parry & Wroth [1981] an expression for α is presented in terms of E_h , E_v , ν_{hh} and ν_{vh} corresponding to equation 5.

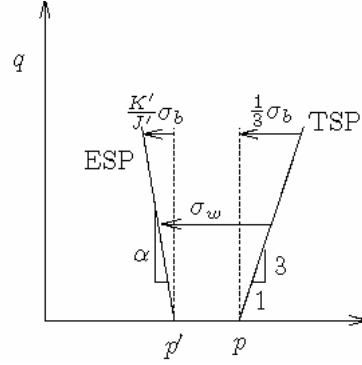


Figure 1 Typical stress path for linear elasticity

3 MEASUREMENTS ON PEAT

Figure 2 shows twelve test results on peat samples collected at the Island of Marken (The Netherlands). The tests have been conducted in order to study dike stability. In total 12 samples are tested. Six were collected at the toe of the dyke and six underneath the dyke. Before the test the samples are consolidated at the level of the original vertical effective stress. Which is approximately 10 kPa for the samples collected at the toe of the dyke and 30 to 40 kPa for the samples collected underneath the dyke. The water content W , density ρ and loss on ignition N , are derived from remaining soil samples. On average $W = 764\%$ and $\rho = 981.6 \text{ kg/m}^3$ for the samples at the toe of the dyke and $W = 502.5\%$ and $\rho = 1008 \text{ kg/m}^3$ for the samples collected underneath the dyke. For N no distinction is made between samples from the toe and underneath the dyke. On average is found $N = 80\%$. These values correspond well to values presented in literature [den Haan et al, 1995].

Figure 2 shows a clear resemblance between the initial part of the measured ESP and the theoretical ESP. The theory described in the previous section assumes linear elastic material behaviour. This assumption can be validated by the $q - \epsilon_a$ diagram. For reference the values for p' and q when an axial strain $\epsilon_a = 2\%$ is reached is indicated in figure 2 by the symbol +. The tests are ended when $\epsilon_a = 15\%$ is reached. The theory described in the previous section explains the test results for the initial stage of the test. Initially, due to the anisotropy of the peat the pore pressure increases. The increase of pore pressure exceeds the increase of isotropic total stress, according to equation 4. This leads to a reduction in effective isotropic stress under an increasing deviator stress. This process continues until the pore pressure approximates the cell pressure. For these conditions the horizontal effective stress reduces to 0 and the stress path curves. It seems that the samples consolidated at a low-pressure fail when reaching the line $q = 3p'$, while the ESP of samples consolidated at a higher pressure tend to follow this line. According to Wood [1990] this line corresponds to the tension cut-off line.

For each test the gradient of the ESP, α , is found by the application of the least squares method in the range of $q = 0$ to 4 kPa. Table 1 presents the results. It is found $K'/J' > 0$ for the tested peat samples except for test 167. As explained in section 2 this indicates that $E_v < E_h$. A larger value for K'/J' is found for

the samples consolidated at a higher stress level. This might suggest that the degree of an-isotropy not only originates from the structure of the fibres, but is also load or stress induced.

Table 1 The K'/J' value, the average value without test 167

test nr	$(K'/J')_\alpha$	test nr	$(K'/J')_\alpha$
47	0.25	102	0.18
57	0.32	135	0.11
78	0.29	152	0.15
85	0.21	160	0.22
86	0.24	167	(-0.06)
96	0.34	175	0.27
average	0.28		0.19

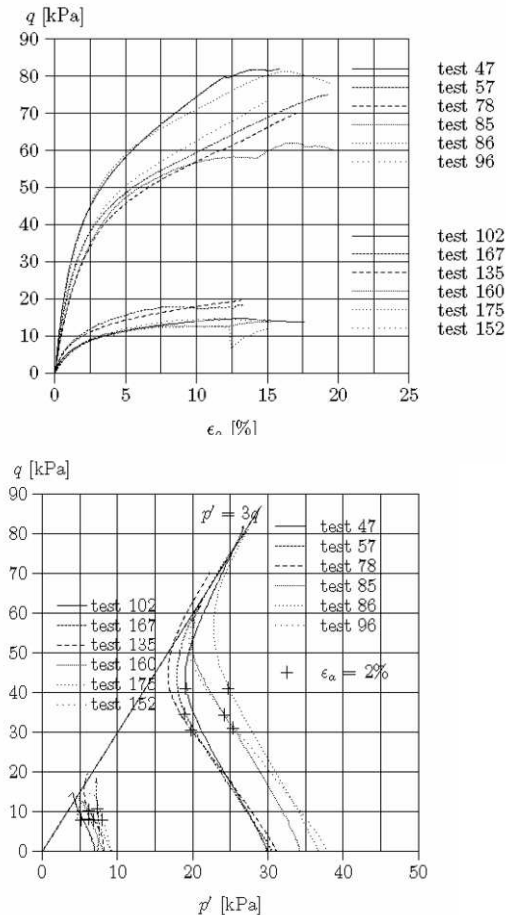


Figure 2 Results of triaxial tests on Marken peat, ϵ_a = axial strain

To verify the findings additional samples are collected at shallow depth underneath an unloaded surface. The location is near Vinkeveen between Utrecht and Amsterdam. At this location the subsoil consists of a 6 m thick peat layer on a thick sand layer. The peat is characterized by $W = 530\%$, $\rho = 1029 \text{ kg/m}^3$ and $N = 53\%$. Samples are retrieved horizontally as well as vertically.

A K0-oedometer [Den Haan & Kamao, 2003] test is run on four samples, 2 on horizontally retrieved samples and 2 on vertically retrieved samples. The tests indicate a pre-consolidation stress of 15.7 and 21.7 kPa for the vertically retrieved samples and 15.9 and 29.3 kPa for the horizontally retrieved samples.

Triaxial tests are run on horizontal and vertically retrieved samples. The samples were consolidated at 10 kPa, so OCR equals approximately 1.5 to 2. Next, a small cycle of axial undrained loading and unloading is applied. To avoid accumulation of pore water a consolidation period is incorporated. Each loading and unloading phase provides information on the axial

stiffness, E_a and the K'/J' value. For the vertically retrieved samples E_a corresponds to the vertical stiffness in the field E_v . While E_a from the horizontally retrieved samples, corresponds to the horizontal stiffness E_h in the field. Next, the samples are consolidated at 20 to 30 kPa and the cycle of undrained loading and unloading phases is applied again. Some samples are re-consolidated at a cell pressure of 10 kPa and the cycle of undrained loading and unloading is applied for the third time. To improve the degree of saturation a backpressure of 300 kPa is used. The degree of saturation is checked by measuring the Skempton B factor. In all tests the Skempton B-factor exceeds 0.98.

Table 2 shows the results. The test conditions are divided in 8 categories. Besides testing horizontally and vertically retrieved samples a deviation is made between loading and unloading phases and tests run at a consolidation stress above or below the pre-consolidation stress in the field. Table 2 shows the axial stiffness derived for the 8 categories. Each loading phase is followed by an unloading phase. For the vertically retrieved samples, the ratio of axial stiffness for the loading phase and following unloading phase equal on average 1.30 and is in the range of 0.8 to 1.95. While for the horizontally retrieved samples this ratio equals 1.31 in the range 0.8 to 1.82.

Table 2 Axial stiffness and K'/J' value for horizontally and vertically retrieved samples, σ'_c = pre-consolidation, H = horizontally retrieved sample, V = vertically retrieved sample, n = number of tests.

H / V	loading / unloading	σ'_c [kPa]	n	E_a [kPa]	K'/J'
V	l	< 20	9	1700 ± 175	0.009
	u	< 20	9	2050 ± 250	-0.021
	l	> 20	2	2047	0.073
	u	> 20	2	3433	-0.017
H	l	< 20	9	1480 ± 400	-0.0982
	u	< 20	9	1715 ± 300	-0.0751
	l	> 20	7	2322 ± 400	0.0591
	u	> 20	6	3130 ± 380	-0.165

The upper and lower boundary values presented in table 2 follows from statistics. As shown by table 2 the difference in loading and unloading stiffness has the same order of magnitude as the difference in horizontal and vertical stiffness for the same loading conditions and consolidation stress. It should be noted that an axial undrained loading causes a radial unloading, while an axial undrained unloading causes a radial loading. So, for a vertically retrieved sample consolidated at 10 kPa, axially loaded has an E_a approximately equal to 1700 kPa and an E_r approximately equal to 1715 kPa. For these conditions the difference in vertical and horizontal stiffness is negligible. The sample is hardly anisotropic, leading to a low value for K'/J' , 0.009 as shown by table 2. A vertically retrieved sample, axially unloaded, shows an E_a of approximately 2050 kPa in combination with an E_r approximately equal to 1480 kPa. With $E_a > E_r$ a negative K'/J' value, -0.021, is found. This corresponds to the theory of section 2. For each set of loading and corresponding unloading phase the vertically retrieved samples the K'/J' value for the unloading phase is smaller then for the loading phase.

For the horizontally retrieved samples, consolidated at 10 kPa, the same reasoning can be followed. However, the radial stiffness of these samples is a combination of the vertical and horizontal stiffness in the field. So the radial stiffness cannot be compared directly to the axial stiffness from the vertically retrieved samples. An axial load on a horizontally retrieved sample combines the low axial stiffness of 1480 kPa to a large radial stiffness of some average value between 2050 and 1715 kPa. This gives $E_a < E_r$ leading to a positive value for K'/J' , according to equation 4. The values for K'/J' found in the tests gives a large scatter. Especially one test, in which three loading – unloading phases at $\sigma'_c < 20$ kPa are tested, gives extreme negative values for K'/J' . Excluding this test from the results

gives a K'/J' equal to 0.028. Unloading of a horizontally retrieved sample combines an E_a of 1715 kPa to an E_r somewhere in the range of 1700 and 1480 kPa leading to a negative value for K'/J' , -0.075 as shown in table 2.

The axial stiffness found at a consolidation stress in the range of 20 – 30 kPa clearly exceeds the axial stiffness found at a consolidation stress of 10 kPa. It can be concluded that the axial stiffness is clearly stress dependant. For the vertically retrieved samples only one cycle of two loading – unloading phases is applied using one sample. Despite the limited number of tests run on vertically retrieved samples at a consolidation stress of 20 – 30 kPa it seems that the axial stiffness of horizontally retrieved samples increases more than axial stiffness of the vertically retrieved sample. Axial loading of a vertically retrieved sample now combines $E_a = 2047$ kPa and an $E_r = 3130$ kPa. The axial and radial stiffness for this condition shows a clear difference and anisotropy is clearly found in the ESP with $K'/J' = 0.073$. Axial unloading of a vertically retrieved sample combines $E_a = 3433$ kPa to $E_r = 2320$ kPa, leading to $K'/J' = -0.017$ which is shown in table 2. The same reasoning explains the values of K'/J' measured for the horizontally retrieved samples consolidated at 20 – 30 kPa.

The values for K'/J' presented in table 2 are clearly below the values presented in table 1, the Marken peat. Soil investigation on the island of Marken shows that the peat layer is approximately 3.5 m thick, at the toe of the dyke, while underneath the dyke the thickness is reduced to 2.1 m. This suggests that the weight of the dyke has compressed the dyke by approximately 40%. To study the effect of large axial compression on the anisotropy of peat one horizontally and one vertically retrieved sample from the Vinkeveen location are axially pre-loaded. At constant cell pressure, 10 kPa, the samples were axially loaded (drained) to 62 kPa for the horizontally retrieved sample and 60 kPa for the vertically retrieved samples. The axial strain at this point is 41% for the horizontally retrieved sample and 38% for the vertically retrieved sample. After unloading and swelling a small deviator stress is applied again to find the E_a and K'/J' value. After unloading and swelling the axial strain is reduced to 29% for the horizontally retrieved sample and 22% for the vertically retrieved sample. Table 3 gives the results.

Table 3 Axial stiffness and K'/J' value for axially pre-consolidated samples.

H/ V	loading unloading	E_a [kPa]	K'/J'
V	loading	1652	0.34
	unloading	1900	0.33
H	loading	1770	0.26
	unloading	-	0.26
H	loading	1770	0.19
	unloading	-	0.31
	unloading	-	-

Table 3 clearly shows that the values for K'/J' increase due to the axial pre-loading. It can be concluded that the relatively large values for K'/J' for the Marken case are dominated by the axial pre-loading in the field caused by the weight of the dyke. This also explains the difference between the samples retrieved underneath the dyke and at the toe of the dyke. Unfortunately, the unloading phase for the horizontally retrieved sample could not be tested due to equipment problems. It is remarkable however that despite the considerable compaction the axial stiffness still falls in the range values found in table 2. The increase in K'/J' which is found in table 3 is then only explained by a considerable increase in radial unloading stiffness. This can be related to the fibrous structure of peat. Initially, unloaded, the fibres have a loose structure. Axial pre-loading causes a considerable axial compaction. Besides the compaction the fibres are stretched in radial direction. This causes a pre-stressing in the radial direction leading to a stiff unloading behaviour in radial direction. So the increase in axial stiffness is accompa-

nied with an even stronger increase in radial unloading stiffness leading to an increase in K'/J'

4 CONCLUSIONS

The ratio K'/J' is a useful parameter when indicating the rate of anisotropy encountered in a triaxial cell test. For non pre-loaded peat samples the rate of anisotropy found in a triaxial test can well be explained by the difference in loading and unloading stiffness. This holds even for (slightly) isotropically overconsolidated samples. The ratio of the axial unloading and loading stiffness is approximately 1.3 for horizontally and vertically retrieved samples for slightly over consolidated as well as for non-over consolidated samples. The axial stiffness strongly depends on the stress level. A large axial compaction increases the rate of anisotropy considerably. The change of anisotropy cannot be explained by a different axial stiffness. Radial pre-stressing of the fibres is a possible reason for the apparent increase in radial unloading stiffness. This explains the difference in the rate of anisotropy found by samples collected underneath a dyke and at the toe of a dyke.

REFERENCES

- Atkinson, J.H., Richardson, D., Stallebras, S.E. (1990) Effect of recent stress history on the stiffness of overconsolidated soil. *Géotechnique* (40)4:531-540
- Atkinson J.H. (2000) Non-linear soil stiffness in routine design 40th Rankine Lecture *Géotechnique* (50)5:487-508
- Den Haan E.J., Kamao S. 2003 Obtaining isotache parameters from a c.r.s. K0-oedometer, *Soils and Foundations* Vol(43)4: 203-214 .
- Den Haan E.J., Uriel A.O., Rafnsson E.A. (1995) Theme report 7 special problems soft soils/soft rocks, in: *The interplay between Geotechnical Engineering and Engineering Geology Proc. 11th European Conf. on Soil M. Foundation Eng*, Copenhagen Vol 9:139-179.
- Graham J., Houlsby G.T.(1983) Anisotropic elasticity of a natural clay, *Géotechnique* (33)2:165-180
- Hird C.C., Pierpoint N.D. (1994) A non-linear anisotropic elastic model for overconsolidated clay based on strain energy, in: *Numerical methods in Geotechnical Engineering*, Smith (ed.) Balkema Rotterdam, ISBN 9054105100
- Hird, C.C., Pierpoint N.D. (1997) Stiffness determination and deformation analysis for a trial excavation in Oxford clay, *Géotechnique* (47)3:665-691
- Lings, M.L. Pennington, D.S. Nash, D.F.T. (2000) Anisotropic stiffness parameters and their measurement in stiff natural clay, *Géotechnique* (50)2:109-125
- Parry, R.H.G., Wroth C.P. (1981) Shear stress strain properties of soft clay. In: *Soft Clay engineering* Brand E.D. & Brenner R.P. ed., Elsevier Amsterdam ISBN 0-444-41784-2
- Wesley, L.D. (1975) Influence of Stress Path and Anisotropy on the behaviour of a Soft Alluvial Clay. Ph.D. Thesis University of London
- Wood, D. M. (1990) Soil Behaviour and Critical State Soil Mechanics. Cambridge University Press, Cambridge ISBN 0-521-33782-8
- Zwanenburg C. Barends F.B.J. (2004) The influence of an-isotropic behaviour on three-dimensional consolidation of soft soil. *5th international PhD symposium in civil engineering*, Walraven, Blaauwendraad, Scarpas & Snijder (eds), Taylor & Francis Group London ISBN 90 5809 676 9